Disorientation Kinetics of Aligned Polymer Layered Silicate Nanocomposites

Jiaxiang Ren, Barbara F. Casanueva, Cynthia A. Mitchell, and Ramanan Krishnamoorti*

Department of Chemical Engineering, University of Houston, Houston, Texas 77204-4004

Received October 1, 2002; Revised Manuscript Received March 10, 2003

ABSTRACT: The kinetics of disorientation of polymer layered silicate nanocomposites following alignment of the silicate layers by prolonged large amplitude oscillatory shear are examined using linear viscoelastic measurements. Nanometer thick disks with diameters of 30 nm, 0.3−0.6 μm, and 5 μm dispersed in polymer matrices exhibit disorientation kinetics that are non-Brownian. The disorientation process exhibits signatures of aging observed in soft-colloidal glasses and is shown to be independent of temperature, nanoparticle size, and chemical details, viscoelasticity and molecular weight of the polymeric matrix.

Introduction

Polymer nanocomposites based on highly anisotropic inorganic nanoparticles such as layered silicates and carbon nanotubes have attracted significant interest.[1,2] The viscoelasticity of such nanocomposites has been extensively studied to determine the changes in polymer dynamics, the influence of the mesoscale structure on the dynamics, and the influence of processing on the material structure and properties of such nanocomposite materials.[2−7] The general conclusions from these studies indicate that the linear viscoelasticity is a sensitive function of the mesoscale dispersion and, to first order, the strength of the polymer−inorganic interaction. On the other hand, the nonlinear (large strain) viscoelasticity is controlled by the ability to orient and align the anisotropic nanoparticles in the flow field. However, depending on the specific applications sought such orientation might be required to be preserved or avoided or performed only along certain directions.

In this paper, we examine the disorientation process under quiescent conditions following alignment (by the application of prolonged large-amplitude oscillatory shear) of layered silicates dispersed in a polymer matrix. Layered silicates employed in this study belong to the class of 2:1 smectites with a layer thickness of 0.95 nm and are organically modified to render them compatible with polymers. The effective disk diameter of the layered silicates ranges from ∼30 nm for Laponite to 0.3−0.6 μm for montmorillonite and ∼5 μm for fluorohectorite. These nanoparticles are dispersed in model polystyrenes (molecular weight ranging from 30K to 290K and with narrow molecular weight distribution) and a model polyisobutylene-based polymer. The nanoscale structures in these nanocomposites range from well-intercalated to disordered intercalated to exfoliated depending on the combination of polymer and layered silicate.

To understand the origins of the disorientation process and the factors controlling it, we systematically explore the role of nanoparticle dimensions and molecular weight and viscosity of the matrix polymer on the disorientation kinetics. Specifically, we wish to examine whether the disorientation is governed by the Brownian motion of the nanoparticles[8,9] or is controlled by cooperative dynamics analogous to those observed in soft colloidal glasses[10−13] or is faster than that expected on the basis of Brownian motion because of potential attraction between the silicate layers.[9,14]

Previous studies of Solomon and co-workers[9] on polypropylene-based montmorillonite exfoliated nanocomposites indicate that the disorientation following alignment is non-Brownian and with disorientation kinetics faster than that predicted by Brownian motion. In that case it was argued that the nanocomposites prepared were intrinsically unstable (thermodynamically), and the strong attraction between the silicates led to the rapid disorientation. On the other hand, Lele and co-workers[14] with in-situ X-ray scattering have suggested that compatibilized syndiotactic polypropylene nanocomposites initially disorient rapidly (much faster than Brownian motion) and then remain at a constant orientation state for a time period of ∼1500 s. It was argued that the rapid initial decrease in the orientation was a result of the coupling of the polymer chains to the silicates and not a result of silicate layer attraction.

Bonn and co-workers[11,15] have recently studied the behavior of aqueous Laponite dispersions using a combination of rheology and dynamic light scattering measurements and have indicated that the recovery following large-amplitude oscillatory preshear demonstrated signatures of cooperative relaxation and exhibiting logarithmic scaling with time. On the other hand, for a similar aqueous dispersion of Laponite with added high molecular weight poly(ethylene oxide), hypothesized to act as dynamic bridges between the Laponite sheets, Han and co-workers[16] have shown that the relaxation following flow-induced alignment is much faster than that expected from Brownian motion and thought to result from the elastic restoring force of the dynamically bound poly(ethylene oxide) chains.

Thus, this brief survey of the literature suggests that the recovery of the microstructure following flow-induced alignment is far from resolved for the case of polymer nanocomposites. In this paper we examine the recovery following large-amplitude oscillatory flow (leading to "parallel" alignment of the layers) for a series of

* To whom correspondence should be addressed. E-mail: ramanan@uh.edu.

10.1021/ma025703a CCC: $25.00
Published on Web 05/08/2003

Table 1. Polymer Characterization

polymer	M_w	M_w/M_n
PS30K; model polystyrene	30 000	<1.06
PS152K; model polystyrene	152 000	<1.06
PS290K; model polystyrene	290 000	<1.06
PIB12K; model random copolymer of isobutylene and *p*-methylstyrene (10 wt % PMS)	12 400	<1.08

thermodynamically and kinetically stable intercalated and exfoliated nanocomposites with nanoparticle disk diameters varying by 2 orders of magnitude and for polymer matrices over a wide range of viscosities and interactions with the silicate layers.

Experimental Section

Three organically modified layered silicates were used: an octadecyl trimethylammonium modified fluorohectorite (C18F), a dioctadecyl dimethylammonium modified montmorillonite (2C18M), and a dioctadecyl dimethylammonium modified Laponite (2C18L). Organic modification was performed using the method described by Giannelis et al.[17,18] In brief, the layered silicates were ion-exchanged using a 5:1 excess of the alkylammonium bromide salt in boiling ethanol−water mixtures and cleaned by repeated refluxive distillation using boiling ethanol followed by filtration to remove all excess alkylammonium. The absence of any excess alkylammonium was ascertained by a silver nitrate test of the supernatant and by thermogravimetric analysis of the cleaned and dried layered silicate. Since the charge exchange capacities (CEC) are different (fluorohectorite, ∼1.5 equiv/kg; montmorillonite, ∼0.9 equiv/kg; Laponite, ∼0.75 equiv/kg), we have employed organic modifications such that the surface coverage of the layered silicates and the conformations of the alkyl modifiers are roughly equivalent, rendering them roughly thermodynamically equal to the intercalation of polymers, at least as interpreted in the mean-field context of the theory of Vaia and Giannelis.[19] By employing a single-stranded surfactant for the high CEC fluorohectorite and a double-stranded surfactant (with the same tail length) for the lower CEC montmorillonite and Laponite, we expect the effects to compensate and render the two organic modifiers to have roughly the same liquidlike conformations prior to intercalation.[17]

The polymers used to prepare nanocomposites include a series of model polystyrenes with narrow molecular weight distribution and obtained from Pressure Chemicals Co. The model poly(isobutylene-*co*-*p*-methylstyrene) (10 wt % PMS) was prepared by living cationic polymerization.[20] The relevant molecular characteristics of the polymers are provided in Table 1.

Nanocomposites were prepared by solution mixing appropriate quantities of polymer and the finely ground layered silicates at room temperature in toluene. The mixtures were allowed to dry at room temperature and subsequently annealed at high temperature in a vacuum oven for an extended period to ensure complete removal of any remaining solvent and facilitate efficient dispersion. X-ray diffraction and transmission electron microscopy measurements indicate that nanocomposites of PS with 2C18M and C18F result in intercalated hybrids with layer center-to-center distance of ∼3 nm. On the other hand, nanocomposites of PIB with 2C18M result in a disordered intercalated nanocomposite while the hybrids of PIB and 2C18L lead to the complete delamination of the stacks of layers.

Melt-state rheological measurements were performed on a Rheometric Scientific ARES rheometer with a torque transducer range of 0.2−2000 g_f cm using 25 mm diameter parallel plates with a sample thickness of 1−2 mm. Linear dynamic oscillatory measurements and prolonged large-amplitude shear to orient samples were used, and the resulting shear stress was interpreted in terms of the in-phase storage modulus (G') and the out-of-phase loss modulus (G''). Additionally, the data were also interpreted in terms of the complex viscosity

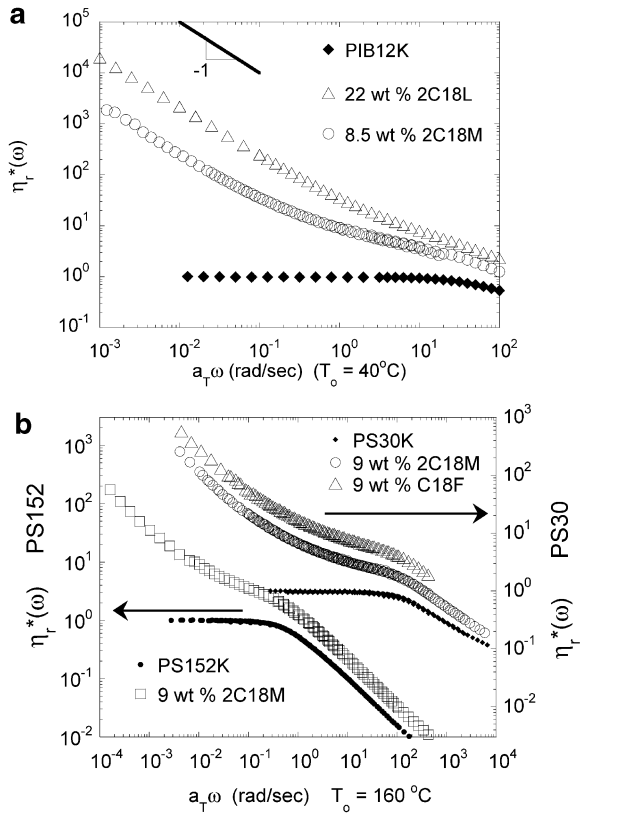

Figure 1. The linear melt-state viscoelastic response of the quiescent state nanocomposites is demonstrated. The data shown are normalized as per eq 1. In (a), the response of two hybrids prepared with the model PIB−PMS copolymer are shown. The hybrids prepared with the 2C18L and 2C18M structurally exhibit a disordered intercalated nanostructure. In (b), the response for nanocomposites based on two different molecular weights (30K and 152K) of PS and 9 wt % 2C18M and C18F are shown. For all samples, the low-frequency data scale as $\omega^{-\alpha}$ ($\alpha \sim 0.9$) consistent with the trends exhibited by aqueous dispersions of Laponite.[11]

η^* ($= \sqrt{G'^2+G''^2}/\omega$). Prolonged large-amplitude oscillatory measurements were carried out until all viscoelastic functions were time independent.

Results and Discussion

The linear dynamic oscillatory viscoelastic measurements for the PIB- and PS-based nanocomposites exhibit solidlike behavior, consistent with the notion that these nanocomposites belong to the general class of soft colloidal glasses. Evidence for this solidlike behavior is presented in Figure 1, where the frequency dependence of the reduced complex viscosity is shown. The reduced linear complex viscosity ($\eta_r^*(\omega)$) is defined as

$$\eta_r^*(\omega) = \frac{\eta^*(\omega)}{\eta_0^\circ} \tag{1}$$

where $\eta^*(\omega)$ is the linear complex viscosity of the sample at a frequency ω and η_0° is the low-frequency Newtonian (complex) viscosity of the pure polymer. The low-frequency behavior, independent of the details of the polymer and the layered silicate, demonstrates a power law behavior with $\eta_r^*(\omega)$ scaling as $\sim\omega^{-\alpha}$, with $\alpha \sim 0.9$ for all the samples examined in this study. This behavior is consistent with the previously mentioned solidlike behavior and is analogous to the behavior of soft colloidal glasses.[11−13] The unique aspect of these

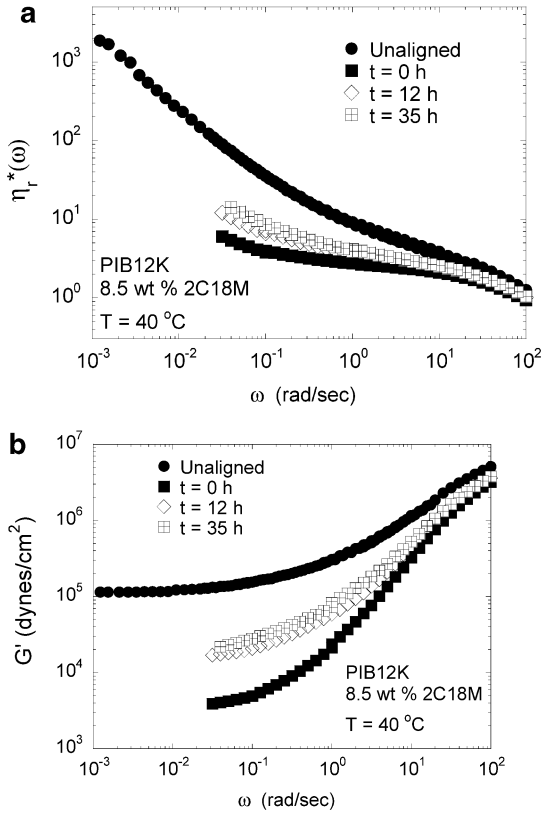

Figure 2. Frequency dependence of the small-amplitude oscillatory viscoelastic response for the unaligned and aligned ($t = 0$) and at intermediate times of quiescent disorientation for the PIB12K-based 2C18M (8.5 wt %) nanocomposite at 40 °C. The data at $t = 0$ were collected immediately following prolonged large-amplitude oscillatory shear (LAOS) at $T = 40$ °C, $\omega = 0.1$ rad/s, and $\gamma_0 = 1.5$ for 16 h.

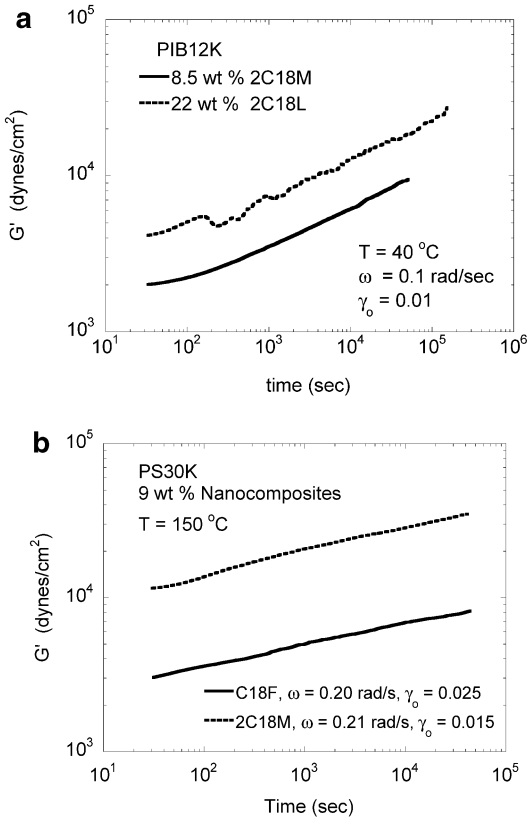

Figure 3. Small-amplitude oscillatory elastic moduli (G') monitoring of the recovery after shear alignment for the PIB12K-based hybrids (a) and for the PS30K based hybrids (b). Recovery measurements were performed at conditions noted in the figures. Alignment for the PIB12K-based hybrids was achieved using alignment conditions detailed in Figure 2. For the PS30K hybrids, alignment was achieved by prolonged LAOS at $T = 180$ °C, $\omega = 0.1$ rad/s, and $\gamma_0 = 1.2$ for 3 h. The value of G' ($\gamma_0 = 1.2$ and $\omega = 0.1$ rad/s at 180 °C) at the end of the LAOS alignment for the C18F and 2C18M nanocomposites are 215 and 940 dyn/cm^2, respectively.

results is the low volume fraction of nanoparticles (~4 vol % for the 2C18M and C18F hybrids and ~9 vol % for the 2C18L-based hybrids), in the absence of electrostatic interactions or strong attractive interactions between the nanoparticles, at which solidlike behavior (and analogy to the behavior of soft colloidal glasses) is observed.

Application of prolonged large-amplitude oscillatory shear leads to the development of aligned samples.[5−7,21] Previously, using small-angle neutron scattering on montmorillonite-based nanocomposites, it has been shown that the predominant alignment of the silicate layers following such a flow history was that of "parallel" layers with layer normals along the velocity gradient direction (see Appendix).[6] Similar results using small-angle X-ray scattering were also obtained by Chen and co-workers[22] on nanocomposites of montmorillonite-filled polystyrene−polyisoprene block copolymers and by Lele and co-workers on polypropylene-based nanocomposites.[14] The small-amplitude oscillatory viscoelastic response following such large-amplitude oscillatory shear is considerably more liquidlike than that prior to flow alignment as shown in Figure 2. Additionally, both η_r^* and G' are significantly smaller (at all frequencies) than those of the unaligned sample. We exploit this significant change in the viscoelastic functions at low frequencies for the aligned and unaligned samples to conveniently probe the kinetics of disorientation (see Appendix for correlation with X-ray scattering measurements).

The kinetics of disorientation for the two nanocomposites based on PIB12K and 2C18L (~30 nm diameter) and 2C18M (0.3−0.6 μm diameter) are presented in Figure 3a. We focus on the linear storage modulus (G') since this viscoelastic function exhibits the largest change between the unaligned and the aligned states. However, similar trends are observed for all viscoelastic functions and at all frequencies as demonstrated by the frequency sweep data at intermediate times of the disorientation process shown in Figure 2. Additionally, the data in Figure 2 and their similarity to data presented in Figure 3 ascertain that the kinetics observed in the continuous low-amplitude shear are not contaminated by the application of this small-amplitude oscillatory shear. Similar data for the disorientation of 2C18M and C18F (5 μm diameter) dispersed in a low molecular weight (30K) PS are shown in Figure 3b. On the basis of the data presented in these figures, the disorientation kinetics exhibit a logarithmic dependence on time ($G' \propto t^{\beta}$, $0.1 \leq \beta \leq 0.25$) irrespective of polymer matrix, layered silicate disk diameter, and effective dispersion of the nanoparticles in the polymer matrix. Compared to the modulus value before shear alignment (Table 2), the moduli values after 50 000 s or more of the recovery are considerably smaller and indicate that the samples are largely aligned even after this time. This conclusion is generally consistent with a recent rheo X-ray study of Lele et al.[14] on a thermodynamically metastable polypropylene-based layered silicate nano-

Table 2. Nanocomposite Disorientation Characteristics

polymer	nanocomposite	temp (°C)	ω ($a_T\omega$)[a] (rad/s)	$G'_{unaligned}(\omega)$ (dyn/cm^2)	D_{r0} (s^{-1})[b]
PS30K	9 wt % 2C18M	135	0.03 (1.77)	6.5×10^5	2.4×10^{-7}
	ref temp = 160 °C	140	0.04 (0.86)	4.6×10^5	6.8×10^{-7}
		150	0.20 (0.86)	4.6×10^5	3.6×10^{-6}
		170	2.62 (0.86)	4.6×10^5	5.8×10^{-5}
PS30K	9 wt % C18F	150	0.20 (0.86)	1.2×10^5	6.2×10^{-9}
	ref temp = 160 °C	170	3.09 (0.86)	1.2×10^5	1.0×10^{-7}
PS152K	9 wt % 2C18M	150	0.03 (0.13)	3.7×10^5	3.3×10^{-8}
	ref temp = 160 °C	165	0.06 (0.03)	1.2×10^5	2.7×10^{-7}
		170	0.03 (8.6×10^{-3})	6.1×10^5	5.1×10^{-7}
		170	0.1 (0.028)	1.1×10^6	5.1×10^{-7}
PS290K	9 wt % 2C18M	170	0.03 (8.6×10^{-3})	3.0×10^5	6.1×10^{-8}
	ref temp = 160 °C	185	0.1 (6.6×10^{-3})	2.8×10^5	2.8×10^{-7}
PIB12K	8.5 wt % 2C18M	40	0.1	4.5×10^5	3.0×10^{-6}
PIB12K	22 wt % 2C18L	40	0.1	1.2×10^6	2.4×10^{-2}

[a] Reduced frequencies reported for the PS are based on a shift to a reference temperature of 160 °C, as noted in column 2. [b] Based on eq 2 and calculated for the case of completely exfoliated single layers.

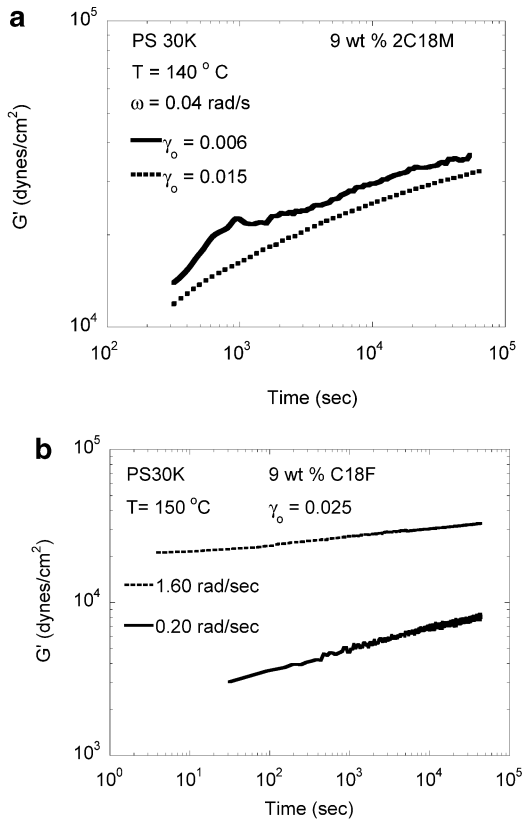

Figure 4. Role of strain amplitude (a) and frequency of measurement (b) on the disorientation kinetics of the PS30K-based nanocomposites. Alignment was achieved using the same conditions reported in Figure 3. The value of G' (γ_0 = 1.2 and ω = 0.1 rad/s at 180 °C) at the end of the LAOS alignment for the data in (a) are 1260 and 1030 dyn/cm^2 for the γ_0 = 0.006 and 0.015 measurements, respectively, and (b) are 160 and 215 dyn/cm^2 for ω = 1.60 and 0.20 rad/s, respectively.

composite system, where the disorientation was examined over much shorter time scales.

The data presented in Figure 3 is largely independent of the strain amplitude during recovery, for small values of the strain amplitude, as demonstrated by representative data in Figure 4a. Similarly, the trends are unchanged for different frequencies at which the recovery is monitored as shown by the representative data in Figure 4b and anticipated on the basis of the frequency scan data for intermediate times presented in Figure 2.

The independence of the disorientation kinetics with nanoparticle size and polymer matrix indicates that the disorientation process is not governed by Brownian motion, where the rotary diffusivity (D_{r0}) of a circular disk of diameter d is[8,23,24]

$$D_{r0} = \frac{3k_BT}{4\eta_0 d^3} \tag{2}$$

where η_0 is the viscosity of the polymer matrix. We choose to model the layered silicate as a circular disk because of the disklike character of individual layers and note parenthetically that the rotary diffusivity of tactoids is comparable to those of the single layers.[8,23,24] Values of D_{r0} based on the case of a single uncorrelated exfoliated layer of the silicate are shown in Table 2. Clearly, for the case of 2C18L and 2C18M, the rotational relaxation time ($1/D_{r0}$) inferred from these values of the idealized rotary diffusivity is smaller or comparable to the experimental time scales. However, the extent of disorientation inferred from the rheological measurements is negligibly small even for those nanocomposites and suggests that the disorientation process is non-Brownian.

To confirm this non-Brownian character of the disorientation process, the matrix viscosity of the polymer was adjusted by changing the temperature of measurement and by changing the molecular weight of the polymer matrix. The data shown in Figure 5 indicate that the matrix viscosity does not significantly alter the trends for the disorientation process. We note that the viscosity changes by about 2 orders of magnitude from 140 to 170 °C for PS30K.[25] For the case of the PS30K in 2C18M and C18F, the reduced frequency and the strain amplitude employed were kept constant in order to facilitate comparisons (Figure 5a,b). In those cases, the disorientation kinetics are not entirely independent of the temperature and might indicate a small coupling to the matrix viscosity. Nevertheless, even at the highest temperature the data after 50 000 s indicate that the modulus (unaligned values in Table 2) and viscosity (η_r*(0.04 rad/s)$_{unaligned}$ ~ 40) have only recovered a small fraction of the original value.

Figure 6 examines the kinetics of disorientation for the nanocomposites prepared with identical amounts of 2C18M dispersed in three different molecular weights of PS compared at roughly the same matrix viscosity (by choice of temperature). As shown in a different paper, increasing the molecular weight of the PS leads

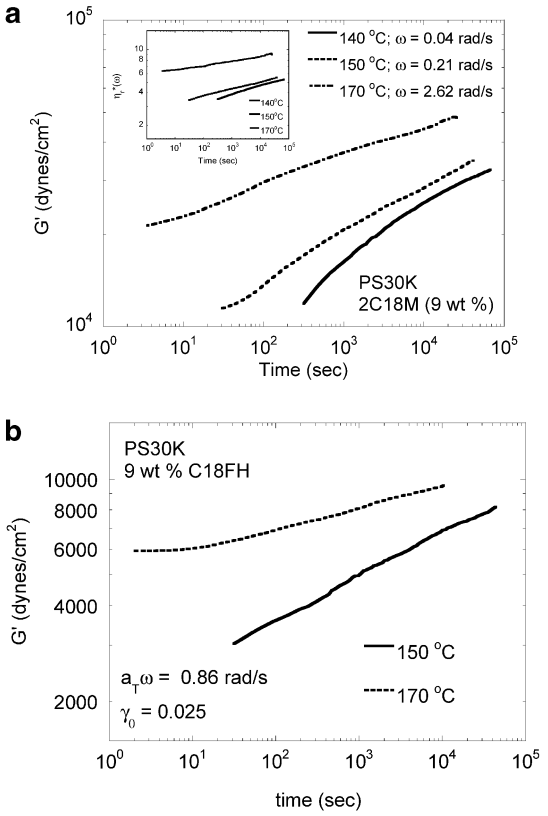

Figure 5. Effect of temperature and matrix viscosity on the disorientation of 9 wt % 2C18M (a) and 9 wt % C18F (b) nanocomposites of PS30K. The matrix viscosity at 140, 150, and 170 °C are measured to be 2.7×10^4, 5.0×10^3, and 3.7×10^2 Pa s, respectively. The relative trends in G' and $\eta_r^*(\omega)$ (shown in inset) with temperature are similar and indicate slightly faster disorientation kinetics at elevated temperatures. The value of G' ($\gamma_0 = 1.2$ and $\omega = 0.1$ rad/s at 180 °C) at the end of the LAOS alignment for the data in (a) are 1030, 940, and 930 dyn/cm^2 for the $T = 140$, 150, and 170 °C measurements, respectively, and (b) are 215 and 195 dyn/cm^2 for $T =$ 150 and 170 °C, respectively.

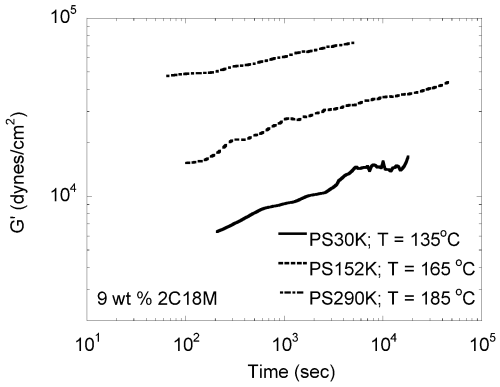

Figure 6. Effect of changing matrix molecular weight on the disorientation kinetics of 9 wt % 2C18M dispersed in polystyrene. Temperatures were chosen to maintain a constant matrix viscosity. The value of G' ($\gamma_0 = 1.0$ and $\omega = 0.1$ rad/s at 180 °C) at the end of the LAOS alignment for the data are 390, 4160, and 20 500 dyn/cm^2 for PS30K, PS152K, and PS290K (LAOS at $T = 185$ °C instead of 180 °C), respectively.

to an improved dispersion of the silicate layers (i.e., larger fraction of individual layers) and argued to result from the increased shear and normal stresses due to the higher molecular weight matrices in these systems.[25] As observed from the figure, the data for the three samples are qualitatively similar and indicate that the matrix molecular weight has a negligible effect on the disorientation process.

Thus, we have conclusively shown that the disorientation after alignment by large-amplitude oscillatory shear exhibits logarithmic scaling with time, does not depend on the dimensions of the silicate layers or their aggregates, the state of aggregation or disaggregation (dispersion) of the silicate layers, and does not depend on the temperature or viscoelasticity or molecular weight of the polymer matrix.

Similar trends (logarithmic scaling of the recovery modulus) have been observed for the spin glasses, microgel pastes, Laponite dispersions, and nematic polymers and have been considered in the context of the analogy to soft colloidal glasses.[11,12,26] For aqueous dispersion of Laponite these trends have been confirmed using both rheological and dynamic light scattering measurements.[11,15]

The original quiescent state structure of the intercalated and exfoliated hybrids consists of randomly oriented layers or tactoids of layers, and this randomly distributed structure forms a sample spanning network structure (possibly mediated by polymer chains) responsible for the linear viscoelastic response observed in Figure 1.[4] Such a structure that is intrinsically disordered and metastable is at the core of the analogy to soft colloidal glasses. Importantly, Brownian forces alone are unable to erase the energy barriers created by such structures. Application of shear is considered to change the energy landscape and allows for the system to access new metastable states.[27] For this reason, the application of large stresses (larger than the yield stress) are considered as rejuvenating conditions and in the context of vitrification can be considered to be analogous to heating above the glass transition temperature.[26] Upon removal of the stress (equivalent to quenching below the glass transition), it is anticipated that the energy landscape is again changed, requiring the system to find a new metastable state consistent with the changed landscape. This recovery from the liquid state shows many similarities to physical aging including the observed logarithmic dependence of the recovery modulus and the independence of the disorientation process from the detailed physical characteristics of the layered silicate and the polymer.

While such an energy landscape-based argument appears to be entirely valid for isotropic particles dispersed in a Newtonian small molecule matrix, the extension of these ideas to highly anisotropic particles is experimentally robust as demonstrated by our results here and those of Bonn et al. on aqueous Laponite dispersions.[11] We note that, unlike the Laponite dispersion case examined by Bonn and co-workers, the layered silicates in our experiments are charge neutral with a stoichiometric amount of the balancing alkylammonium cationic surfactants. Thus, long-range correlations resulting from the ionic interactions of the layered silicates (i.e., edge−edge, edge−face, and face−face interactions) are unlikely to be the driving force for randomization of the silicate layers or their aggregates. Instead, the weak attraction between the polymer and the layered silicate (responsible for the miscibility of the polymer and the layered silicates, the intercalated structure, and the quiescent network structure)[18,19,25] and the geometric restrictions resulting in the network structure and cooperativity possibly provide the driving force for the recovery. The interaction forces between

the polymer and the layered silicate are unlikely to be long-ranged and are not expected to result from osmotic effects where gallery compression or expansion would have accompanied the mesoscale structural changes. Nevertheless, by carefully controlling the thermodynamic interactions (i.e., making them extremely weak or extremely strong) and by probing the disorientation and multitude of length scales (nano to macro), the precise origins of the disorientation processes in these systems can be determined and should be pursued.

Concluding Remarks

The disorientation kinetics of aligned layered silicates (either individual or tactoids of stacked sheets) exhibit non-Brownian character and are not dependent on the physical and chemical parameters of the inorganic nanoparticles and the polymer matrix. These measurements suggest that the postprocessing structure of these materials (after the attainment of layers aligned "parallel") is likely to change slowly with close similarities to physical aging if the polymer matrix is above its softening point. However, it is quite possible that the layers do not necessarily attain parallel alignment and might in fact obtain perpendicular or even transverse alignment after realistic steady shear or elongational processing as suggested by several recent studies.[5,16,28] In those cases, the recovery after flow alignment might be quite different from that observed in the current study.

Acknowledgment. We gratefully acknowledge the ExxonMobil Chemical Company for partial financial support of this work. Useful discussions with Jack Douglas and Richard Vaia are also gratefully acknowledged.

Appendix

To verify the evolution of the microstructure during the quiescent period following large-amplitude oscillatory shear, we conducted ex-situ X-ray measurements of the quenched nanocomposites at different times following the large-amplitude oscillatory alignment. We focused on the PS152K with 9 wt % 2C18M nanocomposites and performed disorientation studies at 170 °C after shear alignment at 180 °C (strain amplitude of 1.5 applied for ~3 h). X-ray measurements were conducted on samples quenched immediately after shear alignment, after 1 h quiescent disorientation at 170 °C, and after 48 h quiescent disorientation at 170 °C in the rheometer under a N_2 environment. As per Table 2, at these conditions of measurement we anticipate a rotary diffusivity of 5×10^{-7} s^{-1}, and in fact over 48 h a significant disorientation would be anticipated on the basis of Brownian disorientation of the layered silicates.

X-ray measurements of small samples (1 mm thickness) prepared with the X-ray beam traveling roughly parallel to the radial direction were performed, and the azimuthal scans of the data in the q range corresponding to the (001) layer−layer registry peak are shown in Figure 7. The as-prepared sample (not subjected to large-amplitude oscillatory flow) demonstrated relatively little preferential orientation of the silicate layers (i.e., random orientation) as would have been expected. On the other hand, the sample oriented after large-amplitude oscillatory shear demonstrated a significant extent of orientation of the sample. Interestingly, the samples held under quiescent conditions at 170 °C for 1 and 48 h show relatively little disorientation of the oriented silicate layers. These results are largely consistent with the qualitative trends described in the paper using linear viscoelastic measurements. However, a direct quantitative comparison was not possible because of the relative difficulty in converting the (unidirectional) orientation function directly to viscoelastic properties.

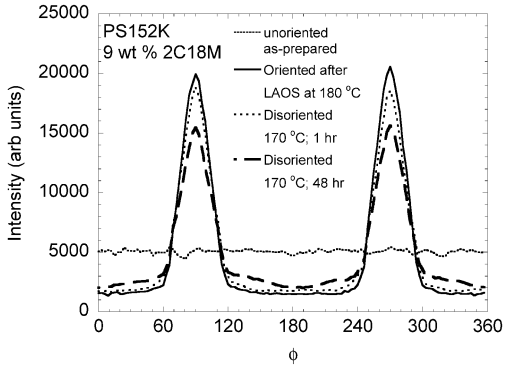

Figure 7. Study of the mesoscale structure using ex-situ two-dimensional X-ray scattering for a 9 wt % 2C18M in polystyrene (152K) as a function of annealing time at 170 °C are shown. The data corresponding to the (001) peak ($q \sim 0.2$ Å^{-1} and $\Delta q = 0.02$ Å^{-1}) were sectioned in 3° increments and shown here. Samples were prepared as disks with sections (~2 × 1 × 1 mm) near the circumference taken and examined with the X-ray beam parallel to the radial direction. The data prior to large-amplitude shear indicate a material that is isotropic. On the other hand, all the other samples indicate an anisotropic material, with the layers predominantly oriented in "parallel" orientation (with layer normals along the velocity gradient direction). After 48 h of quiescent annealing, the sample demonstrates a relatively small amount of disorientation consistent with the rheological findings.

References and Notes

(1) Giannelis, E. P.; Krishnamoorti, R.; Manias, E. *Adv. Polym. Sci.* **1999**, *138*, 107−147. Manias, E.; Touny, A.; Wu, L.; Strawhecker, K.; Lu, B.; Chung, T. C. *Chem. Mater.* **2001**, *13*, 3516−3523. Haggenmueller, R.; Gommans, H. H.; Rinzler, A. G.; Fischer, J. E.; Winey, K. I. *Chem. Phys. Lett.* **2000**, *330*, 219.

(2) Mitchell, C. A.; Bahr, J. L.; Arepalli, S.; Tour, J. M.; Krishnamoorti, R. *Macromolecules* **2002**, *35*, 8825−8830.

(3) Krishnamoorti, R.; Ren, J.; Silva, A. S. *J. Chem. Phys.* **2001**, *114*, 4968−4973. Mitchell, C. A.; Krishnamoorti, R. *J. Polym. Sci., Part B: Polym. Phys. Ed.* **2002**, *40*, 1434−1443.

(4) Ren, J.; Silva, A. S.; Krishnamoorti, R. *Macromolecules* **2000**, *33*, 3739−3746.

(5) Krishnamoorti, R.; Yurekli, K. *Curr. Opin. Colloid Interface Sci.* **2001**, *6*, 464−470.

(6) Krishnamoorti, R.; Silva, A. S. In *Polymer-Clay Nanocomposites*; Pinnavaia, T. J., Beall, G. W., Eds.; John Wiley & Sons: New York, 2000; pp 315−343.

(7) Krishnamoorti, R.; Giannelis, E. P. *Macromolecules* **1997**, *30*, 4097−4102.

(8) Larson, R. G. *The Structure and Rheology of Complex Fluids*; Oxford University Press: New York, 1999.

(9) Solomon, M. J.; Almusallam, A. S.; Seefeldt, K. F.; Somwangthanaroj, A.; Varadan, P. *Macromolecules* **2001**, *34*, 1864−1872.

(10) Derec, C.; Ajdari, A.; Lequeux, F. *Eur. Phys. J. E* **2001**, *4*, 355−361. Lacks, D. J. *Abstr. Pap. ACS* **2001**, *221*, 223-COMP.

(11) Bonn, D.; Tanase, S.; Abou, B.; Tanaka, H.; Meunier, J. *Phys. Rev. Lett.* **2002**, *89*, 015701.

(12) Sollich, P.; Lequeux, F.; Hebraud, P.; Cates, M. E. *Phys. Rev. Lett.* **1997**, *78*, 2020−2023. Sollich, P. *Phys. Rev. E* **1998**, *58*, 738−759.

(13) Fielding, S. M.; Sollich, P.; Cates, M. E. *J. Rheol.* **2000**, *44*, 323−369.

(14) Lele, A.; Mackley, M.; Galgali, G.; Ramesh, C. *J. Rheol.* **2002**, *46*, 1091−1110.

(15) Bonn, D.; Kellay, H.; Tanaka, H.; Wegdam, G.; Meunier, J. *Langmuir* **1999**, *15*, 7534−7536.
(16) Schmidt, G.; Nakatani, A. I.; Butler, P. D.; Karim, A.; Han, C. C. *Macromolecules* **2000**, *33*, 7219−7222.
(17) Vaia, R. A.; Teukolsky, R. K.; Giannelis, E. P. *Chem. Mater.* **1994**, *6*, 1017.
(18) Vaia, R. A.; Giannelis, E. P. *Macromolecules* **1997**, *30*, 7990−7999.
(19) Vaia, R. A.; Giannelis, E. P. *Macromolecules* **1997**, *30*, 8000−8008.
(20) Tse, M. F.; Wang, H.-C.; Shaffer, T. D.; McElrath, M. C.; Modi, M. A.; Krishnamoorti, R. *Polym. Eng. Sci.* **2000**, *40*, 2182−2193.
(21) Krishnamoorti, R.; Giannelis, E. P. *Langmuir* **2001**, *17*, 1448−1452.
(22) Chen, H. Ph.D. Thesis: "Polymer Layered Silicate Nanocomposite: Rheology and Intercalation Kinetics" in Department of Materials Science and Engineering, Cornell University, Ithaca, NY, 2001.
(23) Brenner, H. *Int. J. Multiphase Flow* **1974**, *1*, 195−341.
(24) To describe the dynamics of a finite size tactoid, the rotary diffusivity of a spheroid with aspect ratio p (= a/b, where a and b are the minor and major dimensions of the axissymmetric spheroid) and leading dimension L (= b) is given as[8] $D_{r0} = [3k_BT(\ln(2p) - 0.5)]/\pi\eta_0L^3$. On the other hand, the extensive work by Brenner[23] suggests that the rotary diffusivity of a spheroid is given as $D_{r0} = k_BT\{[3(p^2\alpha_{||} + \alpha_\perp)]/[16\pi\eta ab^2(p^2 - 1)]\}$, where $\alpha_{||} = 2(p^2\beta - 1)/(p^2 - 1)$ and $\alpha_\perp = p^2(1 - \beta)/(p^2 - 1)$ with β for oblate spheroids given as $\beta = (\cos^{-1} p)/[p(1 - p^2)^{1/2}]$. This expression for the rotary diffusivity contains no logarithmic terms. Calculations of the rotary diffusivities for tactoids containing 30 layers[4] (3 nm center-to-center apart) based on the above three expressions indicate that the rotary diffusivity of such tactoids are comparable to (and sometimes larger than) those reported for the single layer disks in Table 2.
(25) Ren, J.; Krishnamoorti, R. *Macromolecules*, to be submitted.
(26) Cloitre, M.; Borrega, R.; Leibler, L. *Phys. Rev. Lett.* **2000**, *85*, 4819−4822.
(27) Lacks, D. J. *Phys. Rev. Lett.* **2001**, *87*, 225502. Gagnon, G.; Patton, J.; Lacks, D. J. *Phys. Rev. E* **2001**, *64*, 051508. Lacks, D. J.; Wienhoff, J. R. *J. Chem. Phys.* **1999**, *111*, 398−401.
(28) Okamoto, M.; Nam, P. H.; Maiti, P.; Kotaka, T.; Hasegawa, N.; Usuki, A. *Nano Lett.* **2001**, *1*, 295−298. Medellin-Rodriguez, F. J.; Burger, C.; Hsiao, B. S.; Chu, B.; Vaia, R. A.; Phillips, S. *Polymer* **2001**, *42*, 9015−9023.

MA025703A